Fine-grained habitat-associated genetic connectivity in an admixed population of mussels in the small isolated Kerguelen Islands

Christelle Fraïsse[1,2,*], Anne Haguenauer[3], Karin Gérard[4], Alexandra Anh-Thu Weber[3,5], Nicolas Bierne[1] and Anne Chenuil[3]

[1] Institut des Sciences de l'Evolution UMR5554, Université Montpellier, CNRS, IRD, EPHE, 34095 Montpellier cedex 05, France.

[2] Institute of Science and Technology Austria, Am Campus 1, 3400 Klosterneuburg, Austria.

[3] Institut Méditerranéen de Biodiversité et d'Ecologie marine et continentale - CNRS UMR 7263, Aix-Marseille Université, Station marine d'Endoume, 13007 Marseille, France.

[4] Laboratorio de Ecosistemas Marinos Antárticos y Subantárticos, Instituto de la Patagonia, Universidad de Magallanes, Avenida Bulnes #01890, Punta Arenas, Chile.

[5] Zoological Institute, University of Basel, Vesalgasse 1, 4051 Basel, Switzerland.

[*] *Corresponding author: E-mail: christelle.Fraïsse@ist.ac.at.*

Running title: Admixture and genetic-environment association in a small island

Keywords: *Mytilus* mussels, Fine-grained connectivity, , Admixture, Introgression, Genetic - environment association.

Abstract

Reticulated evolution -i.e. secondary introgression / admixture between sister taxa- is increasingly recognized as playing a key role in structuring infra-specific genetic variation and revealing cryptic connectivity patterns. When admixture zones coincide with ecological transitions, the connectivity patterns often follow environmental variations better than distance and introgression clines may easily be confounded with local adaptation. The Kerguelen mussels is an ideal system to investigate the potential role of admixture in enhancing micro-geographic structure, as they inhabit a small isolated island in the Southern Ocean characterized by a highly heterogeneous environment. Furthermore, genomic reticulation between Northern species (*M. edulis, M. galloprovincialis* and *M. trossulus*) and Southern species (*M. platensis*: South America and the Kerguelen Islands; and *M. planulatus*: Australasia) has been suspected. Here, we extended a previous analysis by using targeted-sequencing data (51,878 SNPs) across the three Northern species and the Kerguelen population. Spatial structure in the Kerguelen was then analyzed with a panel of 33 SNPs, including SNPs that were more differentiated than the genomic average between Northern species (i.e., ancestry-informative SNPs). We first showed that the Kerguelen lineage splitted very shortly after *M. edulis* and *M. galloprovincialis* initiated speciation, and it subsequently experienced admixture with the three Northern taxa. We then demonstrated that the Kerguelen mussels were significantly differentiated over small spatial distance, and that this local genetic structure was associated with environmental variations and mostly revealed by ancestry-informative markers. Simulations of admixture in the island highlight that genetic-environment associations can be better explained by introgression clines between heterogeneously differentiated genomes than by adaptation from admixture variation.

Introduction

Marine species with planktonic larvae are high-dispersal organisms, with large effective population sizes and living in a highly connected environment (Cowen & Sponaugle 2009), therefore they generally show low levels of genetic differentiation across their species ranges (Palumbi 1992). Nevertheless, there is some evidence that micro-geographic genetic-environment associations occur at specific loci in marine species, such as barnacles (Schmidt & Rand 1999), mussels (Koehn *et al.* 1980) or Atlantic killifishes (Reid *et al.* 2017), despite genome-wide genetic homogeneity. These locus-specific associations are traditionally expected in regions of the species range where environmental gradients promote local adaptation of specific populations (Schmidt *et al.* 2008). Alternatively, genetic-environment associations can be observed where semi-permeable genetic backgrounds form a contact zone that coincides with an ecological boundary (Bierne *et al.* 2011). In this case, reproductive isolation genes become locally coupled with local adaptation genes and linked neutral markers, and the two genetic backgrounds become associated with different habitats. In addition, introgression creates a departure from equilibrium situations in which the influx of heterospecific alleles from one genetic background generates a gradient in allele frequencies within the other genetic background, revealing cryptic connectivity patterns (Gagnaire *et al.* 2015). Gradients of introgression may easily be confounded with local adaptation signatures, especially when environmental variables are better proxy of the connectivity matrix than geographic distance. There are two reasons for that: (i) the environment can have a direct effect on connectivity (e.g. landscape resistance model, Zeller *et al.* 2012), or (ii) the effect of a barrier to dispersal can be better described by one of the many scored environmental variables that can incidentally or truly coincide with it, than by distance. In the sea, regions of little water mixing are inevitably both ecotones and barrier to larval dispersal. Most importantly, the reduction in gene flow between genetic backgrounds is expected to be visible only on a subset of markers either because localized at

an intermediate linkage map distance to reproductive isolation genes (Gagnaire *et al.* 2015) or because of heterogeneous differentiation produced by linked selection (Simon and Duranton 2018). This potential effect of introgression on our capacity to detect connectivity breaks in apparently well-mixed populations is of central concern to conservation and species management (Gagnaire *et al.* 2015).

Mytilus mussels are an excellent system to address these issues, because they are subdivided into partially reproductively isolated species. Moreover, a recent study based on F_{ST} genome scans and gene genealogies demonstrated that population-specific introgression is widespread, and it is the primary cause of outlying levels of genetic differentiation between conspecific populations (Fraïsse *et al.* 2016). *Mytilus* mussels have an antitropical distribution, i.e. they occur in high latitudes of the Northern and Southern Hemispheres, as a result of transequatorial migration during the Pleistocene (Hilbish *et al.* 2000; Gérard *et al.* 2008). In the North, *M. edulis* and *M. galloprovincialis* are closely-related species which started to diverge about 2.5 mya (Roux *et al.* 2014), while *M. trossulus* is an outgroup to them with a divergence dated at 3.5 mya (Rawson & Hilbish 1995). The three species have experienced a complex history of divergence punctuated by periods of gene flow (Roux *et al.* 2014; Fraïsse et al. 2018); and nowadays they display hybrid zones where their ranges overlap (Skibinski *et al.* 1983; Väinölä & Hvilsom 1991; Bierne *et al.* 2003). In the South, a re-evaluation of allozyme data and a review of the results obtained with mtDNA and two nuclear DNA markers (Borsa *et al.* 2012) encouraged to group Southern mussels in two different taxa, namely *M. platensis* for those related to *M. edulis* (the South American and Kerguelen mussels), and *M. planulatus* for those related to *M. galloprovincialis* (the Australasian mussels). The presence of a mitochondrial clade endemic to the Southern Ocean further suggests Southern mussels are native rather than introduced by human-mediated activities (Hilbish *et al.* 2000; Gaitán-Espitia *et al.* 2016).

In the Southern Indian ocean, the isolated Kerguelen Islands harbor *M. platensis* mussels which

are polymorphic for allozyme alleles characteristic of all three Northern species (Blot *et al.* 1988), although they are most similar to *M. edulis* at a few allozyme loci (McDonald *et al.* 1991). Further analyses with nuclear markers strengthened the view of a mixed genome ancestry of the Kerguelen mussels (Borsa *et al.* 2007): at Glu-5', a Northern diagnostic marker, mussels carry a heterospecific polymorphism (*M. edulis* / *M. galloprovincialis*). These preliminary results suggest either that reproductive isolation genes responsible of the interspecific barrier in the North were not yet evolved at the time of admixture (if any) in the Kerguelen, or that isolation is not as strong in the demographic, ecological and genetic context of the Kerguelen Islands as it is in the Northern Hemisphere hybrid zones.

The geomorphology of the Kerguelen Islands has been shaped by volcanic activity and glacial erosion which resulted in a carved coast with sheltered bays and fjords (Gérard *et al.* 2015). Recently, Gérard *et al.* (2015) have investigated the genetic-environment associations in the island with four nuclear markers (mac-1, Glu-5', EFbis and EFprem's) and a mitochondrial gene (COI). Only Glu-5' revealed significant genetic differentiation among and within geographic regions, and between habitats, despite the very small geographical scale. This pattern is striking as intraspecific genetic variation rarely shows significant differentiation even over large distances in *Mytilus* (e.g. within the Mediterranean Sea, Fraïsse *et al.* 2016). In particular, allele frequencies at Glu-5' were associated with the presence/absence of the kelp *Macrocystis* in the island, which serves as substrate and refuge for many species of molluscs, including mussels (Adami & Gordillo, 1999). As such, local adaptation was invoked to explain the fine-scale maintenance of polymorphism at Glu-5’, although alternative interpretations involving admixture could not have been refuted.

Our aim was to investigate whether reticulate evolution actually contributed to micro-geographic structure in the Kerguelen islands. To this end, we ask the following questions: (i) can we detect footprints of introgression from Northern species and disentangle them from incomplete lineage sorting (i.e. shared ancestral polymorphism)? ; (ii) is there genetic differentiation at fine scale in the

114 island?; (iii) is there association of genetic differentiation with environmental variables and/or
115 geography?; (iv) is the signal observed in (ii) and (iii) genome-wide or concentrated on ancestry-
116 informative loci and (v) does introgression contribute to this fine-scale genetic differentiation?
117 Based on published genotyping-by-sequencing (GBS) data of the three Northern species (Fraïsse *et*
118 *al.* 2016) and new GBS data of a sample from a single Kerguelen population, we found that the
119 Kerguelen Islands harbor a Southern lineage of mussels, related to *M. edulis,* and that was
120 subsequently admixed with Northern species. Despite ancient incomplete lineage sorting resolved
121 into multifarious topologies among the four taxa, and despite a non-negligible rate of ongoing
122 sorting of lineages (i.e. true shared ancestral polymorphism), we also robustly detected past
123 introgression events between Northern and Southern mussels by: (i) testing for admixture with
124 genome-wide allele frequency data, (ii) reconstructing gene genealogies at a small chromosomal
125 scale and (iii) inferring their divergence history from the joint site-frequency spectrum. Based on a
126 new panel of SNPs genotyped on 695 mussels across 35 sites in the Kerguelen, we then confirmed
127 using redundancy analysis (RDA) a significant fine-scale genetic differentiation between sites
128 associated with environmental variables. Notably, we found that loci with strong genetic-
129 environment association also tended to be among the most ancestry-informative markers in the
130 *Mytilus spp*. While we cannot refute whether local adaptation has played a role here, simulations of
131 admixture in the island highlights the importance of introgression for the current and local genetic
132 structure of the Kerguelen mussels.

133 Materials and Methods

134 Genotyping-by-sequencing of the *Mytilus* spp.

135 We used samples collected from nine localities in the Northern Hemisphere (Figure 1, Supp. Info.
136 M&M and Table S1) to investigate the patterns of admixture between Northern and Southern

genetic backgrounds in the Kerguelen Islands. The genetic composition of these samples has been analysed in Fraïsse *et al.* (2016) with target enrichment sequencing of bacterial artificial chromosomes (BAC) and cDNA sequences (see Supp. Info. M&M for details). The Northern samples have been shown to be representative of monospecific panmictic patches of the *Mytilus edulis* species complex, which comprise three species that hybridize at several places in the Northern Hemisphere: *M. galloprovincialis*, *M. edulis* and *M. trossulus*. In addition to these previously published samples, eight individuals from the Kerguelen Islands (Baie de la Mouche, Table S1) were included in the target enrichment experiment. These individuals were treated together with the Northern samples following the genotyping-by-sequencing (GBS) method described in Fraïsse *et al.* (2016) (see Supp. Info. M&M for details). The final dataset across the ten localities consisted of 1,269 reference sequences (378 BAC contigs that come from a pool of 224 unlinked clones, and 891 cDNA contigs that correspond to unlinked coding sequences of known-functions or randomly selected) and 129,346 SNPs. DNA sequences and VCF files including GBS genotypes are available on Dryad doi: 10.5061/dryad.6k740 (Fraïsse *et al.* 2016).

KASPar SNP panel

Based on the SNP database generated by GBS, we specifically selected SNPs segregating in the eight GBS-typed Kerguelen individuals to analyse the fine-scale genetic structure in the island, and its relation to the local environment. Moreover, as we wanted to determine if the micro-geographic structure in the Kerguelen was primarily driven by standing variation in the Northern complex of species (i.e. SNPs fixed between Northern species), the selected SNPs were not a random sample of the SNPs detected by GBS, otherwise they would have been mainly private polymorphisms to the Kerguelen (60% of the Kerguelen SNPs were found private). As such, we further enriched our SNP array with ancestry-informative markers, the most differentiated SNPs between pairs of Northern Hemisphere species (representing 33% of the non-private Kerguelen SNPs, 10% of the whole SNP

161 dataset), namely the West-Mediterranean *M. galloprovincialis* population, the North-Sea *M. edulis*
162 population and the Baltic-Sea *M. trossulus* population. F_{ST} values (Weir & Cockerham 1984) were
163 calculated using the R package hierfstat (Goudet 2005) for each SNP between pairs of populations
164 (Text S1). SNPs in the upper 15% of the empirical F_{ST} distribution were categorized as highly-
165 differentiated. SNPs with more than 25% of missing data were discarded. SNPs were further
166 filtered-out based on Illumina Assay Design Tool scores (available on Illumina web page,
167 http://support.illumina.com) which predicts probes success based on the number of degenerated
168 sites in the flanking sequences (250 bp on each side of the focal SNP). The final array comprised 58
169 SNPs out of which 30 were highly differentiated between Northern species (11 *M. trossulus*-
170 specific, 8 *M. edulis*-specific and 10 *M. galloprovincialis*-specific, Table S2).

171 **KASPar genotyping in the Kerguelen Islands**

172 We used samples collected from 35 sites in the Kerguelen Islands by Gérard *et al.* (2015), totalling
173 695 individuals (Supp. Info. M&M and Table S3). We additionally included other samples from the
174 Southern Hemisphere (Gérard *et al.* 2008) to assess the genetic relationships previously proposed
175 by Borsa *et al.* (2012) with a handful of markers: one sample from Western Australia in Nedlands
176 (AUS, n=12 individuals); two samples from New Zealand, Dunedin (DUN, n=8) and Wellington
177 Harbour (WHL, n=10); two samples from Tasmania, the Simpson's Bay (SIM, n=8) and Hobart
178 (HOB, n=9); one sample from Chile in Maullin (MAU, n=15). Pieces of mantle tissue were
179 preserved in 95% ethanol, and DNA was extracted with the Macherey-Nagel NucleoSPin 96 Tissue
180 kit. We used KASPar (Kompetitive Allele Specific PCR, Smith & Maughan 2015), a fluorescence-
181 based genotyping assay of allele-specific PCR products, to genotype the 58 SNPs, of them, 44 SNPs
182 were successfully amplified. We removed seven loci which showed significant F_{ST} values between
183 the eight GBS-typed Kerguelen individuals and the KASPar individuals. These may be due to error
184 in the genotyping-by-sequencing, typically the assembly of paralogous loci in two alleles of the

185 same locus, or alternatively to problem of amplification in the KASPar assay as a consequence of
186 primer design. More generally, these discrepancies call for studies that quantitatively compare the
187 two genotyping methods. We further eliminated two loci with null alleles (significant F_{IS} values in
188 most of the sampling sites) and two loci physically linked to one another. The final dataset was
189 composed of 33 KASPar SNPs (Table S2). Additionally, we included allele frequency data of a
190 length-polymorphism locus in the adhesive plaque protein gene, Glu-5', previously scored in the
191 same sampling sites (Gérard *et al.* 2015). Genotypes for all individuals at each KASPar SNP is
192 available in Text S2, and population allele frequencies are given in Table S4.

193 **Genetic network of the *Mytilus* spp.**

194 Genotypes of the GBS dataset were statistically phased with beagle v3.3.2 (Browning & Browning
195 2007) using genotype likelihoods provided by bcftools. All individuals were included in the analysis
196 to maximize linkage disequilibrium, and 20 haplotype pairs were sampled for each individual
197 during each iteration of the phasing algorithm to increase accuracy. Phased sequences (haplotypes)
198 were then generated using a custom perl script. An individual genetic network analysis was
199 conducted with splitstree4 v4.12.6 (Hureson & Bryant 2006) to get insight into the population
200 relationships across the three Northern Hemisphere species and the eight individuals sampled in the
201 Kerguelen Islands. All haplotype loci were compiled to create a composite chromosome of 51,878
202 high-quality SNPs and analysed using the neighbour-net method.

203 **Analyses of admixture in the *Mytilus* spp.**

204 An estimation of the historical relationships among the nine Northern populations and the GBS-
205 typed Kerguelen population was performed with *TreeMix* v.1.1 (Pickrell & Pritchard 2012).
206 TreeMix jointly estimates population splits and subsequent admixture events based on the F-
207 statistics introduced by Reich *et al.* (2009), and commonly recognised as a valid support for
208 admixture (e.g., in humans: Pickrell & Pritchard 2012, Wong *et al.* 2017). A maximum-likelihood

population tree was estimated based on the matrix of GBS allele frequency covariance between population pairs, and admixture events were sequentially added. To account for linkage disequilibrium, variants were grouped together in windows of size k=100 SNPs. Trees were rooted with the two *M. trossulus* populations and no sample size correction (option "-noss") was applied. We tested for a range of migration events from m=0 to m=12, and looked for an asymptotic value of the log-likelihood. The number of significant migration events was assessed by stepwise comparison of Akaike information criterion. Finally, we made 100 bootstrap replicates (option "–bootstrap") of the maximum-likelihood tree to assess statistical support of migration events.

Based on the GBS genotypes, we additionally performed a model-based clustering analysis of these populations, which assumes admixed individuals with contributions from *K* panmictic reference populations. Ancestry of each individual was estimated using the maximum-likelihood approach implemented in ADMIXTURE v1.23 (Alexander *et al.* 2009). We ran 50 replicates for a number of clusters from K=2 to K=8 and chose the maximum log-likelihood run for each K. We also performed a supervised ADMIXTURE analysis (in which the reference populations were provided) on the Kerguelen individuals with the KASPar SNPs (K=2 clusters and 50 replicates). We defined *M. edulis* and the *M. platensis* Chilean mussels as ancestral populations from which the Kerguelen individuals derive their ancestry. Individual ancestries are provided in Text S3 for the GBS analysis and Text S4 for the KASPar analysis.

In complement to the *TreeMix* analysis, we used a model-based approach implemented in ∂a∂i v1.6.3 (Gutenkunst *et al.* 2009) to explicitly test for the presence of gene flow. This method has proven useful for distinguishing ancestral shared polymorphism between recently-diverged species evolving under strict isolation from a scenario including migration between them (e.g., in *Arabidopsis*: Hubert *et al.* 2014; sea bass: Tine *et al.* 2014; poplars: Christe *et al.* 2017; whitefish: Rougeux *et al.* 2017). We assessed the divergence history between Kerguelen mussels and Northern species in a pairwise manner based on their folded joint site frequency spectrum at the cDNA

9

contigs (provided in Text S5 in ∂a∂i format, and plotted in Figure S1): Kerguelen vs. *M. edulis* (represented by the European sample "EU – peripheral"); Kerguelen vs. *M. galloprovincialis* (Mediterranean sample "MED – west"); Kerguelen vs. *M. trossulus* (European sample "EU"). We defined fourteen demographic models following previous studies (Tine *et al.* 2014; Christe *et al.* 2017) to test: (i) the timing of gene flow during divergence (absence of gene flow "SI", continuous migration "IM", secondary contact "SC", ancient migration "AM", periodic secondary contact "PSC" with two periods of current gene flow, periodic ancient migration "PAM" with two periods of ancient migration, and a three-period model of ancient migration, isolation and current gene flow "AMSISC"); (ii) the genomic heterogeneity in gene flow (presence "2M" or absence of interspecific genomic barriers); (iii) the genomic heterogeneity in effective population size (presence "2N" or absence of Hill-Robertson effects). All models began with the split of the ancestral population in two daughter populations, and then were followed by divergence in the absence or presence of gene flow. Each model was fitted to the observed joint site frequency spectrum (singletons were masked) using three successive optimization steps: "hot" simulated annealing, "cold" simulated annealing and BFGS -Broyden–Fletcher–Goldfarb–Shanno- algorithm (Tine *et al.* 2014). Model comparisons were made using Akaike information criterion. A summary of the models is given in Table S5 and the script that defines the models in ∂a∂i is given in Text S6.

Topology weighting of the *Mytilus* spp.

The distinct haplotype loci of the GBS dataset were also individually analysed with the neighbour-net method. Allele genealogies were inferred with the R package APE (Paradis 2010) using a neighbour-joining algorithm with F84 distances (Felsenstein & Churchill 1996). Haplotype loci were filtered based on the following excluding criteria: scale < 0.00005 ; 0.00005 =< scale < 0.0005 & length < 10000 bp ; 0.0005 =< scale < 0.001 & length < 5000 bp ; and scale >= 0.001 & length >= 1000 bp, where "scale" is the scale of the gene tree and "length" is the length of the sequence.

10

258 Neighbour-joining trees of the 395 retained sequences are available in Text S7 and their length are
259 indicated in Table S6 (4.5 kb in average, a minimum length of 1 kb and a maximum length of 25
260 kb).

261 For each haplotype locus, the relationships between the Northern species and the Kerguelen
262 population were then quantified using *Twisst*, a tree weighting approach that has been successfully
263 applied to *Heliconius butterflies* to evaluate the support of different phylogenies around colour
264 pattern loci (Van Belleghem *et al.* 2017). We tested the three possible unrooted topologies: (A) *M.*
265 *edulis* grouped with the Kerguelen population; (B) *M. galloprovincialis* grouped with the Kerguelen
266 population and (C) *M. trossulus* grouped with the Kerguelen population. Their exact weightings to
267 the full tree were estimated by considering all subtrees ("complete method"). Only contigs with a
268 resolved topology were analysed: 67 contigs for which one topology had a weight greater or equal
269 to 0.75. These topologies were further classified in two categories depending on whether they most
270 plausibly reflect: (i) ancient divergence of the Kerguelen population (i.e. the Kerguelen and
271 Northern individuals clustered into distinct monophyletic groups) or, (ii) introgression with one of
272 the Northern species (i.e., the Kerguelen individuals were distributed within one or more Northern
273 clades); "na" stands for topologies that we were unable to classify in these two categories due to a
274 lack of informative sites. Tree topology weightings and classification are available in Table S6.

275 **Analyses of genetic variation in the Kerguelen Islands**

276 For each KASPar SNP, estimation of F_{ST} values (Weir & Clark Cockerham 1984) was calculated
277 over all sampling sites (Table S2), and in a pairwise manner across all SNPs (Table S7) using
278 Genetix 4.05 (Belkhir *et al.* 2002). Their significance was tested by a permutation procedure (1000
279 permutations) and adjusted with the Bonferroni's correction for multiple comparisons (Benjamini &
280 Hochberg 2000).

281 **Analysis of habitat variables in the Kerguelen Islands**

To evaluate how much of the genetic variation among sites was explained by local environmental factors, we used redundancy analysis (RDA), a constrained ordination method implemented in the R package vegan (Oksanen *et al.* 2017). It performs a multiple linear regression between a matrix of response variables (individual genotypic data) and a matrix of explanatory variables (environmental factors). Notably, the effect of partially confounded explanatory variables can be estimated separately. RDA is commonly used to estimate the relative contribution of spatial and environmental components on species communities, and it has been recently applied to analysis of population genetic structure (e.g., Legendre & Fortin 2010). Geographic coordinates and five qualitative factors were measured in each site to describe the local habitat (Table S3): (i) Substrate (rock: R, blocks: B, gravels: G, or sand: S); (ii) Wave Exposure (sheltered: Sh, or exposed: E); (iii) Slope (flat: F, steep: St, or hangover: H); (iv) Salinity (oceanic water: OW, or low-salinity water: LSW); (v) *Macrocystis* (presence: P, or absence: A).

We specifically tested the effect of each of these constrained factors (explanatory variables) on the distribution of genotypes at the 33 KASPar SNPs (response variables). The following initial model was used: Genotypes ~ *Macrocystis* + Salinity + Slope + Exposure + Substrate + Longitude + Latitude. The significance of the global model was first established by permutation test, in which the genotypic data were permuted randomly and the model was refitted (1000 permutations). Marginal effect permutation tests were then performed to assess the significance of each factor by removing each term one by one from the model containing all other terms (1000 permutations). Non-significant factors were removed from the final model. Based on that simplified model, we performed a conditioned RDA analysis for each factor to assess its contribution to the genotypic variance independently from the other explanatory variables. These co-variables were removed from the ordination by using a condition function: Genotypes ~ tested variable + condition(all other variables). Finally, we performed a conditioned RDA on geography to specifically control its confounding effect: Genotypes ~ significant environmental variables + condition(significant

12

307 geographic variables).

308 **Simulations of secondary contact**

309 Following the methodology of Gagnaire *et al.* 2015, we modelled a secondary contact between two
310 semi-isolated genetic backgrounds (*M. edulis* vs. *M. platensis* Chilean population) that meet twice
311 on a circular stepping stone model of 30 demes (between demes n°18 / n°19 and demes n°19 /
312 n°20), and start to exchange genes. At generation zero, the *M. edulis* background settles in deme
313 n°19 while the *M. platensis* background is located everywhere else. Their initial allele frequency at
314 the barrier loci was set-up to 0.10 for the *M. edulis* background and 0.70 for the *M. platensis*
315 background, which correspond to the average foreign allele frequency at the four most
316 differentiated loci observed in the *M. edulis* and Chilean *M. platensis* mussels, respectively (see
317 Figure 4B). The auto-recruitment rate was set to 1-*m*, and migration to adjacent demes was *m*/2
318 (with *m*=0.5). A barrier to dispersal was set between demes n°18 and n°19 (*m*=0.05), which
319 corresponds to the genetic break observed between sites PAF and RdA in the Kerguelen Islands.
320 Selection acts in haploid individuals on a two-locus incompatibility, which is linked to a neutral
321 marker located 1cM away and unlinked to a second neutral marker. Strong and asymmetric
322 selection were required to maintain the two genetic backgrounds after contact (s=0.5 against the *M.*
323 *platensis* allele in the *M. edulis* background vs. s=0.2 against the *M. edulis* allele in the *M. platensis*
324 background). Deme size was constant and set to 500 individuals.

325 **Results**

326 **The Kerguelen mussels: signal of divergence of a Southern lineage after transoceanic**
327 **migration and admixture with Northern lineages**

328 An individual genetic network (Figure 1) was built from a subset of 51,878 high-quality SNPs

329 genotyped in nine Northern populations and eight individuals from the Kerguelen Islands. We
330 observed that the Northern populations formed three distinct clusters, corresponding to the three
331 Northern species: *M. edulis*, *M. galloprovincialis* and *M. trossulus*. Accordingly, the majority of
332 SNPs fixed between populations (295 in total) were species-specific: *M. edulis*=6, *M.*
333 *galloprovincialis*=62 and *M. trossulus*=224. The Kerguelen individuals clustered together into a
334 single clade. Indeed, the proportion of SNPs which were private to the Kerguelen Islands amounted
335 to 60% (3,805 private for a total of 6,297 SNPs in Kerguelen, after removing singletons). In
336 comparison, the number of private SNPs in *M. trossulus* was 3,070, and it was only 492 in *M.*
337 *galloprovincialis* and 48 in *M. edulis* (indicative of introgression between the two latter species).
338 Among the 2,492 SNPs shared by the Kerguelen mussels with Northern species, 33% (830) were
339 highly differentiated between at least two Northern species. When considering Northern species-
340 specific SNPs, 83% of those fixed in *M. edulis* were segregating in the Kerguelen (5 for a total of 6
341 fixed). These numbers were 16% for *M. galloprovincialis* (10 for a total of 62 fixed) and 12% in *M.*
342 *trossulus* (27 for a total of 224 fixed). A multivariate analysis on KASpar-typed SNPs, including the
343 Northern samples, the Kerguelen Islands and other samples from the Southern Hemisphere that
344 were also genotyped in our SNP assay, is provided as a supplementary figure (Figure S2). The
345 principal component analysis clearly shows that the Chilean mussels (MAU) group with the
346 Kerguelen mussels in accordance with them being both named *M. platensis*; while the Australasian
347 samples (Australia, Tasmania and New-Zealand), usually named *M. planulatus*, cluster with the
348 Northern *M. galloprovincialis*. These findings corroborate previous results based on mitochondrial
349 DNA (Gérard *et al.* 2008) and nuclear markers (Borsa *et al.* 2012).

350 The species relationships found in the genetic network (Figure 1) were generally supported by the
351 maximum-likelihood population tree inferred by *TreeMix* (Figure 2A), except that the Kerguelen
352 population was inferred as the sister-group of *M. edulis*. The pairwise population residuals in a
353 model without admixture (Figure S3) suggested substantial migration between species. So, we

354 sequentially allowed from 0 to 12 migration events in the analysis, and assessed their significance
355 by stepwise comparison of Akaike information criterion (Figure S3). The best fit to the data was
356 obtained with seven migration events, which significantly improved the log-likelihood of the model
357 (Figure S3). This population tree was bootstrapped 100 times to assess statistical support of
358 migration events. They were generally weakly supported, with only four migration events that had
359 more than 50% bootstrap support (Figure 2A and Table S8). The most robustly inferred migration
360 event was between the Mediterranean *M. galloprovincialis* and the Kerguelen population (81 % of
361 bootstrap replicates). The two others included migration among Northern species as expected: the
362 European populations of *M. edulis* and *M. galloprovincialis* (51%), and the European populations of
363 *M. edulis* and *M. trossulus* (68%). Migration events were also inferred between the Mediterranean
364 *M. galloprovincialis* and the European *M. trossulus* (55%), as well as between the Kerguelen
365 population and the American *M. trossulus* (38%). Reticulated evolution with the American *M.*
366 *trossulus* was further supported by their excess of privately shared polymorphism with the
367 Kerguelen population (Figure 2B). Migration between the Kerguelen population and the European
368 *M. edulis* was detected, but only in 4% of bootstrap replicates.

369 Our reconstruction of the divergence history with ∂a∂i consolidated evidence for admixture
370 between the Kerguelen mussels and each Northern species, although pointed out to a periodic
371 connectivity with several periods of admixture. In all three comparisons, the models without gene
372 flow were consistently the worst supported ("Strict Isolation", Table S5). In the *M. edulis* and *M.*
373 *galloprovincialis* comparisons, the model of periodic ancient migration with varying rates of
374 introgression among loci ("*PAM_2M*") received the strongest statistical support (Table S5).
375 Migration occurred right after the split as well as later in the divergence during a relatively short
376 period (~15% to 25% of the total divergence time) and it was asymmetric with a substantial fraction
377 (85% to 90%) of the mussel genome in the Kerguelen permeable to *M. edulis* and *M.*
378 *galloprovincialis* gene flow. In the *M. trossulus* comparison, the three-period model with

379 homogeneous rates of introgression among loci ("AMSISC") was the best supported (Table S5). A
380 first period of ancient migration lasted ~85% of the divergence time, and was followed by a short
381 period of isolation and a very short secondary contact (~2% of the total divergence time). Kerguelen
382 mussels were mostly resistant to *M. trossulus* introgression (Table S5). Overall, these results suggest
383 that the Kerguelen mussel is a Southern lineage related to *M. edulis* and that it admixed with all
384 three Northern species (*M. edulis*, *M. galloprovincialis* and to a lesser extent with *M. trossulus*) in
385 the past, either after secondary contact and/or early in the divergence of the species.

386 **Variation of admixture histories across the genome**

387 To further investigate how genetic relationships varied across the genome, we quantified the
388 contribution of three unrooted topologies (Figure 3) to the full tree at 395 GBS contigs with *Twisst*.
389 Only 17% (67) of them showed resolved relationships, i.e. one of the unrooted topology weighted
390 75% or more, among which 40% (27) were highly resolved (weight >= 90%). The reason for this
391 low rate of resolved relationship is twofold: (i) ongoing sorting of shared ancestral polymorphism,
392 and (ii) introgression. In the Northern Hemisphere introgression has been shown to be the main
393 process thanks to model fitting (Fraïsse *et al.* 2018) and using comparison of introgression
394 differential between populations within species (Fraïsse *et al.* 2016). It is more difficult to tell apart
395 ancestral shared polymorphism from introgression for the single Kerguelen population. Above
396 analyses suggest introgression is contributing although it is difficult to evaluate its contribution. The
397 most represented resolved topology (39 contigs) put the Kerguelen individuals together with *M.*
398 *edulis*, while they were grouped with *M. trossulus* in 19 contigs (i.e. ancestral to the *M. edulis* / *M.*
399 *galloprovincialis* subgroup) and with *M. galloprovincialis* in 9 contigs (Table 1). This illustrates a
400 high rate of ancient incomplete lineage sorting that resolved into alternative topologies after the
401 consecutive speciation events, which resulted in the three species *M. edulis*, *M. galloprovincialis*
402 and *M. platensis*. In other words, the transequatorial migration that leads to *M. platensis* occurred
403 soon after the split between *M. edulis* and *M. galloprovincialis*.

When classifying the topologies in categories, 18 contigs supported the "ancient Kerguelen divergence" scenario while 19 supported an "introgression" scenario among which 4 were from *M. trossulus*, 12 from *M. edulis* and 3 from *M. galloprovincialis*; 30 contigs could not be classified. It should be noted that all these patterns hold when using a minimal weight of 90% (Table 1). Figure 3 illustrates representative cases of the different *Twisst* categories, including candidate loci for introgression (A2, B2 and C2 in Figure 3). These results suggest that the Kerguelen mussels have a genome of mixed ancestry, mainly dominated by *M. edulis,* from which they are closely-related, but with which they also have probably secondarily admixed. This is in accordance with the *TreeMix* analysis where the Kerguelen population was inferred to be the sister-clade of *M. edulis* and experienced admixture events with *M. edulis* and *M. galloprovincialis*. However, this seems quantitatively different from the ∂a∂i results in which both *M. edulis* and *M. galloprovincialis* broadly contributed to the genomic composition of the Kerguelen mussels. However, we call for caution when comparing these two methods as ∂a∂i provides genome-wide migration rate estimates, while *Twisst* relies on counting different types of topologies across the genome and many gene trees could not be classified, and *TreeMix* infer single admixture event under the hypothesis of homogeneous introgression (while *Mytilus* species barriers are often semi-permeable, Roux *et al.* 2014, Fraïsse *et al.* 2018, and see Table S5).

Substantial genetic structure in the Kerguelen Islands

Mussels were collected from 35 sampling sites all around the Kerguelen Islands (Figure 4A, Table S3) and successfully genotyped at 33 KASpar SNPs. Pairwise F_{ST} values across all SNPs (Table S7) revealed significant fine-scale genetic differentiation between sites from different geographic regions. Remarkably, RdA (North-East) and PCu (West) were significantly differentiated with nearly all other sites. Sites from the South, especially BdS, and from the North, especially AS, were differentiated from the Gulf of Morbihan. At a smaller scale within the Gulf of Morbihan, genetic

17

structure among several sites was detected, but their significance level did not pass the correction for multiple tests. These results extend the study by Gérard *et al.* (2015) to many SNPs and substantiate their finding of significant genetic differentiation at different scales in the island.

Global F_{ST} across all sites was calculated for each SNP and tested with 1000 permutations (Table S2). Values were non-significant after Bonferroni's correction, except at the three most differentiated loci, which are ancestry-informative: X10, X11 and X57. Their foreign allele, defined based on its frequency in the Northern species (*M. galloprovincialis* Atlantic population of Iberian Coast, Table S4), was at low frequency in the North of the island, especially in the North-East sites, RdA and PMo. In contrast, it was at higher frequency in the Gulf of Morbihan and at intermediate to low frequency in the South and West. These trends were similar to those at Glu-5' (Table S4), a nuclear marker suspected to be affected by differential selection in the island (Gérard *et al.* 2015) and at candidate allozymes although with fewer sampling sites (Blot *et al.* 1989). Across all sites, the frequencies of the foreign allele at Glu-5' were significantly correlated with those at X10 ($r=0.61$, p-value < 0.001), X11 ($r=0.419$, p-value=0.012), and X57 ($r=0.49$, p-value=0.003), but they were globally higher at Glu-5' (Figure S4).

The foreign allele frequency at those four loci is represented in Figure S4 and the average over the four loci in Figure 4B (filled symbols). These clearly show a genetic break between two geographically close sites, PAF and RdA (40 kms apart), and to a lesser extent between RdA and Pmo, which are separated by only 8 kms of coasts. The average frequency was the highest in the Gulf of Morbihan (from HdS to PAF), then it abruptly dropped down (in 40 km) between PAF and RdA (respectively on the West and East coast of the Prince of Wales' Peninsula), and finally increased gradually along the coast from North-East to South-West. Notably, the variance in allele frequency at the four loci was weak (0.0208 in average across localities). This is in sharp contrast with the pattern observed at the other loci (open symbols) of which the average frequency remained similar across all sites (Figure 4B), and variance was stronger (0.0938 in average across localities).

18

453 An admixture analysis using all KASPar SNPs and defining *M. edulis* and the Chilean mussels as
454 reference populations (Figure 4B, pie charts), suggests that the Kerguelen Island is occupied by
455 mussels related to Chilean mussels (*M. platensis*), and that RdA has by far the highest level of *M.*
456 *edulis* ancestry (31% compared to <19% elsewhere). We therefore hypothesize that two genetic
457 backgrounds may be present in the island, one related to *M. edulis* and trapped at site RdA close to a
458 potential density trough in the the Prince of Wales' Peninsula, and the other related to Chilean
459 mussels and present everywhere else. This pattern is theoretically expected (Barton 1979, Barton &
460 Hewitt 1985) as areas of low density or low carrying capacity tend to trap "tension zones" between
461 incompatible genetic backgrounds (similarly to ecological boundaries).
462 We illustrated this scenario by simulating a secondary contact between these two backgrounds
463 (including a physical barrier to dispersal between demes n°18 and n°19), and tracking the frequency
464 of the foreign allele at two neutral markers (linked and unlinked to the barrier locus) a few hundreds
465 generations after the contact (Figure 4C). Simulations often fitted well with the observed variation
466 in allele frequency across sites, as predicted by Gagnaire *et al.*'s model (2015), provided that the
467 species barrier was asymmetric in order to protect *the small* M. edulis patch to be quickly swamped
468 by *M. platensis* introgression. This suggests that the genetic break at the boundary of the Gulf of
469 Morbihan and the North-East region is better revealed by the frequency of foreign alleles at
470 ancestry-informative loci implying a role of admixture either in the maintenance or in the detection
471 of the genetic structure.

472 **Environment-associated genetic structure in the Kerguelen Islands**

473 We then tested for genetic-environment associations in the Kerguelen by performing a RDA.
474 Among the seven constrained factors (five qualitative variables, plus geographic coordinates), three
475 were not significant in the initial model (Salinity, Exposure and Latitude, Table S9) and were
476 removed from further analyses. The proportion of total genotypic variance explained by all

477 constrained factors was highly significant in the global model (p-value=0.001, Table 2A, left panel),
478 but quite low (2.32%). The first RDA axis, which explained 61% of the constrained variance, was
479 mainly contributed by *Macrocystis* presence/absence (Figure S5 and Table S10). Accordingly, it was
480 the only factor whose marginal effect remained significant (p-value=0.032, Table 2B, left panel).

481 We statistically controlled for the effect of geography by performing a conditioned RDA analysis
482 on Longitude (Table 2A, right panel). The combined effect of the three environmental variables
483 remained significant (p-value=0.041), explaining 1.1% of the total genotypic variance. Individually,
484 *Macrocystis* presence/absence and Substrate still showed significant effects, after removing all other
485 confounding factors (p-value=0.011 and 0.001, respectively, Table 2B, right panel). This suggests a
486 limited effect of geography on the genetic structure of the mussels, although coastal distance would
487 be a better proxy to account for spatial structure in the island. Interestingly, it has been previously
488 shown that the fine-scale genetic variation at Glu-5' was also significantly associated with
489 *Macrocystis* presence/absence (Gérard *et al.* 2015). Accordingly, we found a significant correlation
490 between the average foreign allele frequency at the four most differentiated loci in the Kerguelen
491 Islands and the presence/absence of *Macrocystis* (Figure 5A), whereas there was no correlation with
492 the other loci (Figure 5B).

493 The sharp genetic break between RdA and PAF further indicates that two genetic backgrounds
494 may have been locally trapped by an ecological boundary or a region of reduced dispersal (Bierne
495 *et al.* 2011). Accordingly, there is an oceanic threshold at the entrance of the Gulf of Morbihan that
496 impedes exchanges with water masses from outside; and at a larger scale, the Antarctic circumpolar
497 current moves the water masses from West to East causing gyres and turbulences on the North-
498 Eastern coast and pushing water masses far to the East (Karin Gerard, pers. comm.). Thus, the water
499 masses between the Gulf of Morbihan and the North Coast do not mix well, suggesting that
500 exchanges between the two sites are limited. Moreover, these two sites differ at all five ecological
501 variables (Table S3), but not in the direction predicted by their geographical origin: RdA shows an

habitat characteristic of the Gulf of Morbihan while being located on the East coast and having the lowest foreign allele frequency (and the reverse is true for PAF). This imperfect association between genotypes and habitats supports the hypothesis that enhanced genetic drift and intense gene flow in the island grambled the signal of genetic-environment association at our markers rather than environmental differential selection.

Most differentiated SNPs in the Kerguelen Islands are primarily ancestry-informative in the Northern Hemisphere

In the total sample, the average allele frequency of the foreign allele was 0.417 at Glu-5', 0.503 at X10, 0.619 at X11 and 0.480 at X57. These polymorphisms were well-balanced in the island (i.e. close to 0.5 frequency), despite being species-specific in the Northern species (Table S2, also see Gérard *et al.* 2015 for Glu-5'). To investigate whether micro-geographic structure in the island was primarily depending on Northern ancestry-informative loci, we compared the degree of differentiation between sites in the Kerguelen Islands and that of the Northern species, *M. edulis* and *M. galloprovincialis*, at the 33 KASPar SNPs (Figure 6). Figure 6A shows that the level of genetic differentiation among sites in the Kerguelen (global F_{ST}, Table S2) was significantly higher (p-value=0.021) for the ancestry-informative loci (mean=0.015, in orange) compared to the background loci (mean=0.007, in grey). Importantly, the difference between the two categories was also significant when considering the genetic-by-environment association across all variables (Figure 6B: mean_orange=0.112, mean_grey=0.048, p-value=0.006), which was measured by the locus coordinates on the first axis of the conditioned RDA (Table S11); or only including *Macrocystis* presence/absence (Table S12: mean_orange=0.089, mean_grey=0.041, p-value=0.016). Moreover, these patterns hold when adding the locus Glu-5' (Figure S6) in the case of genetic differentiation (Figure S6A, p-value=0.01), and genetic-environment associations (Figure S6B, p-value=0.004) measured by the F_{CT} from an AMOVA analysis performed by grouping sites according

21

526 to the presence/absence of *Macrocystis* (see Gérard *et al.* 2015).

527 **Discussion**

528 In this work, we first analyzed the genetic relationship of the Southern Hemisphere Kerguelen
529 mussels with the three Northern species (*M. edulis*, *M. galloprovincialis* and *M. trossulus*) at 1,269
530 contigs (51,878 SNPs), and we confirmed with this large dataset that mussels in the Kerguelen
531 Islands belong to a Southern lineage (*M. platensis*). We further showed that the Kerguelen
532 population is a sister clade of *M. edulis*.

533 Our population tree inference provides evidence of genetic exchanges with Northern mussels that
534 occurred after the first establishment in the Southern Hemisphere. This was confirmed by
535 reconstructing their divergence history, which further suggested that introgression occured at
536 variable rates across the genome with some genomic regions resistant to gene-flow while others are
537 essentially permeable. The resulting genome-wide ancestry variation was estimated by applying a
538 new topology weighting method to each GBS sequence (Martin & Van Belleghem 2016), which
539 weighted the contribution of three topologies to the full tree. The majority of the genome showed
540 evidence for both ancient incomplete lineage sorting, which resolved into alternative topologies
541 among the four species studied *(M. trossulus*, *M. edulis*, *M. galloprovincialis* and *M. platensis*), and
542 shared polymorphisms due to ongoing incomplete lineage sorting and introgression among North
543 Hemisphere species and with the Southern lineage, and this resulted in only 17% of the regions with
544 a well-resolved topology. In 51% of these resolved regions, we found clear evidence of admixture,
545 i.e., the Kerguelen haplotypes were all (or part of) nested within a Northern clade. We thus
546 confirmed that the reticulated evolution of the Southern Hemisphere Kerguelen mussels, which was
547 suggested by a handful of nuclear markers (Borsa *et al.* 2007) and mitochondrial DNA (Hilbish *et*
548 *al.* 2000; Gérard *et al.* 2008), holds at a genome-wide scale. This is in line with recent genomic

549 studies (e.g., *Anopheles gambiae* mosquitoes : Fontaine *et al.* 2015 ; *Xiphophorus* fishes : Cui *et al.*
550 2013 ; African lake cichlids : Meier *et al.* 2017 ; Caribbean *Cyprinodon* pupfishes: Richards &
551 Martin 2017 ; *Heliconius* butterflies : Martin *et al.* 2013) that recognized a prominent role of
552 introgressive hybridization as a source of reticulate phylogenies, besides ancestral shared
553 polymorphism.

554 At some GBS loci, Kerguelen mussels possessed alleles characteristic of both *M. edulis* and *M.*
555 *galloprovincialis* or *M. trossulus* indicating polymorphism for Northern species-specific alleles in
556 the Kerguelen. Importantly, these loci did not depart from Hardy-Weinberg and linkage equilibrium
557 as shown by an ADMIXTURE analysis (Figure S7) in which the Kerguelen mussels appeared as a
558 well demarcated panmictic cluster. Therefore, contrary to what is known in Northern hybrid zones
559 (Bierne *et al.* 2003), there is no evidence of reproductive barriers impeding admixture in the
560 Kerguelen Islands. Several hypotheses can be proposed: (i) a weaker reproductive barrier between
561 Northern backgrounds at the time of contact in the South; or (ii) an insufficient barrier to gene flow
562 under the demographic and environmental conditions, specifically strong genetic drift, high-
563 potential for hybridization in this small isolated island, or a strong demographic asymmetry between
564 the native and the introduced populations. The first hypothesis relies on the importance of
565 Dobzhansky-Müller incompatibilities for reproductive isolation (Coyne & Orr 2004), and may
566 explain how *M. edulis*, *M. galloprovincialis* and *M. trossulus* alleles at different loci can co-exist
567 into a single Southern population that did not evolve their incompatible interactors, as opposed to
568 the Northern populations. The second hypothesis is based on the fact that the outcome of
569 hybridization can be highly dependent on the demographic context.

570 Finally, by collecting mussels from contrasted habitats, we demonstrated significant
571 differentiation across 35 sampling sites at the scale of the island, and at a smaller scale between
572 geographically close sites, especially within the Gulf of Morbihan. As found by Gérard *et al.* (2015)
573 at Glu-5', and previously at allozyme loci (Blot *et al.* 1989), the strongest structure was observed

between the North-South coasts and the Gulf of Morbihan, with a genetic break between RdA and PAF at the three most differentiated loci. The fine-scale genetic structure observed in such a high-dispersal species as mussels is at first sight at odds with selective neutrality. So, we explicitly tested the role of habitat heterogeneity in explaining this differentiation. Our RDA analysis shows that genetic variation was associated with habitats, even after controlling for spatial effects; and the most important factors were the presence of *Macrocystis* kelps, substrate type and slope. Despite being low, this significant habitat-driven genetic differentiation could suggest a role of selection. Another caveat is that spatial distance between sampling sites may be better described by oceanographic distance than geographic coordinates, and so we may be overestimating the influence of habitats.

Firstly, genetic-environment associations could be due to local adaptation of the mussels opposed by gene flow between habitats. Accordingly, we observed a significant correlation between the presence/absence of *Macrocystis* and the average foreign allele frequency at the four most differentiated loci. This points toward a primary effect of *Macrocystis* presence/absence, which is a keystone species in marine ecosystems that forms kelp forest serving as substrate and refuge for many molluscs species, including *Mytilus* (Adami & Gordillo, 1999), in areas exposed to wave action. Nevertheless, the RdA site, which has the lowest foreign allele frequency, is not occupied by *Macrocystis* kelp, weakening this local adaptation hypothesis.

Alternatively, the consistent genetic patterns observed across several physically unlinked loci indicate the possible existence of two genetic backgrounds maintained at the scale of the island. We propose, and illustrate by simulations, that a genetic background related to *M. edulis* is trapped at RdA and surrounded by another genetic background related to Chilean *M. platensis* mussels and present everywhere else. The enclosed location of the genetic background at RdA explains that it is strongly introgressed at most markers and thus hard to detect. However, the physical barrier to dispersal between sites PAF and RdA produces a clear genetic break on the West side of the contact. Introgression between the two backgrounds generates gradients in allele frequencies, which are

24

599 better correlated with habitat variation than geographical distance. The foreign allele (as defined by
600 its frequency in the *M. galloprovincialis* Atlantic population of Iberian Coast) tended to be at higher
601 frequency in shallow sites sheltered from the influence of open marine waters with a low salinity
602 and flat-sandy bottoms, mainly in the inner part of the Gulf of Morbihan. These sites are
603 characterized by an absence of *Macrocystis* kelp beds, as opposed to exposed rocky shores. Port aux
604 Français (PAF) is also the harbour where ships arrive and it is the best place for the arrival of non-
605 native genetic backgrounds. Interestingly, *M. galloprovincialis* alleles are found more frequent in
606 exposed, rather than sheltered sites in the hybrid zone between *M. edulis* and *M. galloprovincialis* in
607 Europe, which would suggest inverted genetic-environment associations between hemispheres.
608 Inverted genetic-environment associations are predicted by the coupling hypothesis (Bierne *et al.*
609 2011), which proposes that genetic-environment associations can easily be revealed by intrinsically
610 maintained genetic backgrounds in linkage disequilibrium with local adaptation genes, and that the
611 phase of the disequilibrium can reverse when contacts are replicated as could have happened in
612 Southern Hemisphere mussels. Overall, these findings reinforce the idea that genetic variation can
613 be maintained at fine geographical scales in high-dispersal organisms, as recently shown in Chilean
614 mussels (Araneda *et al.* 2016) or in passerine birds (Szulkin *et al.* 2016, Perrier *et al.* 2017). In these
615 examples however the link with a possible history of admixture has not been investigated.
616 Although we had the hypothesis that admixture events could be an explanation of the micro-
617 structure observed in the Kerguelen (Gérard *et al.* 2015), we could not know which backgrounds
618 were in interaction on the sole basis of the GBS data of a single sample. However, our procedure of
619 identifying SNPs that were both polymorphic in the Kerguelen and highly differentiated between
620 Northern Hemisphere species proved to be an interesting way to enrich for loci able to reveal the
621 micro-geographic structure in the Kerguelen. Luckily the sample we used for the GBS analysis
622 (sample "ker-GBS") was localised in the introgression cline, and this can also explain why the
623 enrichment procedure was successful. This is exemplified with the genealogy around locus X10

624 (Figure S8), which shows that a SNP that differentiates *M. edulis* from other Northern species, and
625 was polymorphic in the Kerguelen Islands, is able to reveal the cline of introgressed heterospecific
626 allele we observed in the island.

627 In this work, we showed that the most differentiated SNPs in the Kerguelen and those that most
628 strongly drive the genetic-environment associations are primarily ancestry-informative, suggesting
629 that maintenance of genetic differentiation at a small spatial scale, and possibly adaptation to fine-
630 scale environmental variations in the island, may have been facilitated by admixture and
631 introgression of alleles from Northern species. These foreign alleles may have adaptively
632 introgressed the Southern background in the Kerguelen, but the signal is probably erasing because
633 of recombination between adaptive alleles and our neutral markers, and is also probably further
634 blurred by genetic drift. A central question is whether admixture is a simple source of variation on
635 which local selection can effectively act or if the initial linkage disequilibria between foreign alleles
636 in the donor background are required for the successful emergence of micro-geographic adaptation
637 (or speciation in the case of cichlids, Meier *et al.* 2017) and are maintained rather than built-on. In
638 the case of Kerguelen mussels, the evidence we gained here for the maintenance of linkage
639 disequilibrium are limited and indeed rather support extensive recombination. However our markers
640 have likely lost too much signal to answer the question. Maybe local adaptation is operating at loci
641 linked to the candidate SNPs, but most probably these markers simply better reveal a genome-wide
642 signal of habitat constrained connectivity (Gagnaire *et al.* 2015). Overall, our work underlines the
643 opportunity of using non-equilibrium introgression clines to assess genetic connectivity in natural
644 populations and warns against systematically interpreting genetic-environment association as signal
645 of local adaptation.

26

Acknowledgements

Jean-Pierre Féral and Christian Marschal provided the eight Kerguelen specimens used for GBS during the PROTEKER campaign (Programme IPEV n°1044). Other Kerguelen samples (>600) were collected during scientific program IPEV-MACROBENTHOS n° 195 (1999-2003) by the technical volunteers (VATs) from IPEV missions 49–53 in Kerguelen. This work was funded by the Research Network GDR 3445 cnrs ifremer MarCo and the Agence Nationale de la Recherche (HYSEA project, ANR-12-BSV7-0011). This is article 2015-130 of Institut des Sciences de l'Evolution de Montpellier.

References

Adami ML, Gordillo S (1999) Structure and dynamics of the biota associated with *Macrocystis pyrifera (*Phaeophyta) from the Beagle Channel, Tierra del Fuego. *Sci. Mar.*, 63(S1), 183–191.

Alexander DH, Novembre J, Lange K (2009) Fast model-based estimation of ancestry in unrelated individuals. *Genome Res.*, 19, 1655–1664.

Araneda C, Larraín MA, Hecht B, Narum S (2016) Adaptive genetic variation distinguishes Chilean blue mussels (*Mytilus chilensis*) from different marine environments. *Ecol. Evol.*, 6, 3632–3644.

Barton NH, Hewitt GM (1985) Analysis of hybrid zones. *Annu. Rev. Ecol. Evol. Syst.*, 16(1), 113–148.

Barton NH (1979) The dynamics of hybrid zones. *Heredity*, 43(3), 341.

Belkhir K, Borsa P, Chikhi L, Raufaste N, Bonhomme F (2002) GENETIX 4.03, Logiciel Sous Windows Pour la Génétique Des Populations. Laboratoire Génome, Populations, Interactions: CNRS UMR. 5000. Université Montpellier 2, Montpellier, France.

Benjamini Y, Hochberg Y (2000) On the Adaptive Control of the False Discovery Rate in Multiple Testing with Independent Statistics. *Journal of educational and Behavioral Statistics*, 25, 60–83.

Bierne N, Welch J, Loire E, Bonhomme F, David P (2011) The coupling hypothesis: why genome scans may fail to map local adaptation genes. *Mol. Ecol.*, 20, 2044–2072.

Bierne N, Borsa P, Daguin C, Jollivet D, Viard F, Bonhomme F, David P (2003) Introgression

27

patterns in the mosaic hybrid zone between *Mytilus edulis* and *M. galloprovincialis*. *Mol. Ecol.*, 12, 447–461.

Blot M, Thiriot-Quiévreux C, Soyer J (1988) Genetic relationships among populations of *Mytilus desolationis* from Kerguelen, *M. edulis* from the North Atlantic and *M. galloprovincialis* from the Mediterranean. *Mar. Ecol. Prog. Ser.*, 44, 239–247.

Blot M, Thiriot-Quivreux C, Soyer J (1989) Genetic differences and environments of mussel populations in Kerguelen Islands. *Polar Biol.*, 10, 167–174.

Borsa P, Rolland V, Daguin-Thiébaut C (2012) Genetics and taxonomy of Chilean smooth-shelled mussels, *Mytilus spp.* (Bivalvia: Mytilidae). *Comptes rendus biologies*, *335*(1), 51–61.

Borsa P, Daguin C, Bierne N (2007) Genomic reticulation indicates mixed ancestry in Southern-Hemisphere *Mytilus* spp. mussels. *Biol. J. Linn. Soc.*, 92, 747–754.

Browning SR, Browning BL (2007) Rapid and accurate haplotype phasing and missing-data inference for whole-genome association studies by use of localized haplotype clustering. *Am. J. Hum. Genet.*, 81, 1084–1097.

Christe C, Stölting KN, Paris M, Fraïsse C, Bierne N, Lexer C (2017) Adaptive evolution and segregating load contribute to the genomic landscape of divergence in two tree species connected by episodic gene flow. *Mol Ecol*, 26, 59–76.

Cowen RK, Sponaugle S (2009) Larval Dispersal and Marine Population Connectivity. *Annu. Rev. Mar. Sci.*, 1, 443–466.

Coyne JA, Allen Orr H (2004) Speciation. Sinauer Associates Incorporated.

Cui R, Schumer M, Kruesi K, Walter R, Andolfatto P, Rosenthal GG (2013) Phylogenomics reveals extensive reticulate evolution in *Xiphophorus* fishes. *Evolution*, 67, 2166–2179.

Felsenstein J, Churchill GA (1996) A Hidden Markov Model approach to variation among sites in rate of evolution. *Mol. Biol. Evol.*, 13, 93–104.

Fontaine MC, Pease JB, Steele A *et al.* (2015) Mosquito genomics. Extensive introgression in a malaria vector species complex revealed by phylogenomics. *Science*, 347, 1258524.

Fraïsse C, Roux C, Gagnaire P-A, Romiguier J, Faivre N, Welch JJ, Bierne N (2018) The divergence history of European blue mussel species reconstructed from Approximate Bayesian Computation: the effects of sequencing techniques and sampling strategies. *PeerJ*, 6:e5198.

Fraïsse C, Belkhir K, Welch JJ, Bierne N (2016) Local interspecies introgression is the main cause of extreme levels of intraspecific differentiation in mussels. *Mol. Ecol.*, 25, 269–286.

Gagnaire P-A, Broquet T, Aurelle D, Viard F, Souissi A, Bonhomme F, Arnaud-Haond S, Bierne N (2015) Using neutral, selected, and hitchhiker loci to assess connectivity of marine populations in the genomic era. *Evol. App.*, 8, 769–78

28

Gaitán-Espitia JD, Quintero-Galvis JF, Mesas A, D'Elía G (2016) Mitogenomics of southern hemisphere blue mussels (Bivalvia: Pteriomorphia): Insights into the evolutionary characteristics of the *Mytilus* edulis complex. *Sci. Rep.*, 6, 26853.

Gérard K, Bierne N, Borsa P, Chenuil A, Féral J-P (2008) Pleistocene separation of mitochondrial lineages of *Mytilus* spp. mussels from Northern and Southern Hemispheres and strong genetic differentiation among southern populations. *Mol. Phylogenet. Evol.*, 49, 84–91.

Gérard K, Roby C, Bierne N, Borsa P, Féral JP, Chenuil A (2015) Does natural selection explain the fine scale genetic structure at the nuclear exon Glu-5′ in blue mussels from Kerguelen? *Ecol. Evol.*, 5, 1456–1473.

Goudet J (2005) hierfstat, a package for r to compute and test hierarchical F-statistics. *Mol. Ecol. notes*, 5, 184–186.

Gutenkunst RN, Hernandez RD, Williamson SH, Bustamante CD (2009) Inferring the Joint Demographic History of Multiple Populations from Multidimensional SNP Frequency Data. PLOS Genetics 5(10), e1000695.

Hilbish TJ, Mullinax A, Dolven SI, Meyer A, Koehn RK, Rawson PD (2000) Origin of the antitropical distribution pattern in marine mussels (*Mytilus spp*.): routes and timing of transequatorial migration. *Mar. Biol.*, 136, 69–77.

Huber CD, Nordborg M, Hermisson J, Hellmann I (2014) Keeping it local: evidence for positive selection in Swedish *Arabidopsis thaliana*. *Mol. Biol. Evol.*, 31(11), 3026–3039.

Koehn RK, Bayne BL, Moore MN, Siebenaller JF (1980) Salinity related physiological and genetic differences between populations of *Mytilus edulis*. *Biol. J. Linn. Soc.*, 14, 319–334.

Legendre P, Fortin MJ (2010) Comparison of the Mantel test and alternative approaches for detecting complex multivariate relationships in the spatial analysis of genetic data. *Mol. Ecol. Resour.*, 10(5), 831–844.

Martin SH, Dasmahapatra KK, Nadeau NJ, Salazar C, Walters JR, Simpson F, Blaxter M, Manica A, Mallet J, Jiggins CD (2013) Genome-wide evidence for speciation with gene flow in *Heliconius* butterflies. *Genome Res.*, 23, 1817–1828.

Martin SH, Van Belleghem SM (2016) Exploring evolutionary relationships across the genome using topology weighting. *Genetics*, 206, 429-438.

McDonald JH, Seed R, Koehn RK (1991) Allozymes and morphometric characters of three species of *Mytilus* in the Northern and Southern Hemispheres. *Marine Biol.*, 111, 323–333.

McGuire G, Wright F (2000) TOPAL 2.0: Improved Detection of Mosaic Sequences within Multiple Alignments. *Bioinformatics*, 16(2), 130–134.

Meier JI, Sousa VC, Marques DA, Marques DA, Selz OM, Wagner CE, Excoffier L, Seehausen O (2017) Demographic modelling with whole-genome data reveals parallel origin of similar

Pundamilia cichlid species after hybridization. *Mol. Ecol.*, 26, 123–141.

Oksanen J, *et al.* (2017) vegan: Community Ecology Package. R package version 2.4-2. https://CRAN.R-project.org/package=vegan

Palumbi SR (1992) Marine speciation on a small planet. *Trends Ecol. Evol.*, 7, 114–118.

Paradis E (2010) pegas: an R package for population genetics with an integrated-modular approach. *Bioinformatics,* 26, 419–420.

Perrier C, Lozano del Campo A, Szulkin M, Demeyrier V, Gregoire A, Charmantier A (2017) Great tits and the city: distribution of genomic diversity and gene - environment associations along an urbanization gradient. *Evol. App*., doi:10.1111/eva.12580

Pickrell JK, Pritchard JK (2012) Inference of population splits and mixtures from genome-wide allele frequency data. *PLoS Genet.*, 8, e1002967.

Rawson PD, Hilbish TJ (1995) Evolutionary relationships among the male and female mitochondrial DNA lineages in the *Mytilus edulis* species complex. *Mol. Biol. Evol.*, 12, 893–901.

Reid NM, Jackson CE, Gilbert D, Minx P, Montague MJ, Hampton TH, Helfrich LW, King BL, Nacci DE, Aluru N, Karchner SI, Colbourne JK, Hahn ME, Shaw JR, Oleksiak MF, Crawford DL, Warren WC, Whitehead A (2017) The landscape of extreme genomic variation in the highly adaptable Atlantic killifish. *Genome Biol. Evol.*, 9(3), 659–676.

Richards EJ, Martin CH (2017) Adaptive introgression from distant Caribbean islands contributed to the diversification of a microendemic adaptive radiation of trophic specialist pupfishes. *PLoS Genet.* 13(8), e1006919.

Rougeux C, Bernatchez L, Gagnaire PA (2017) Modeling the multiple facets of speciation-with-gene-flow toward inferring the divergence history of lake whitefish species pairs (*Coregonus clupeaformis*). *Genome Biol. Evol.,* 9(8), 2057–2074.

Roux C, Fraïsse C, Castric V, Vekemans X, Pogson GH, Bierne N (2014) Can we continue to neglect genomic variation in introgression rates when inferring the history of speciation? A case study in a *Mytilus* hybrid zone. *J. Evol. Biol.*, 27, 1662–1675.

Schmidt PS, Rand DM (1999) Intertidal microhabitat and selection at mpi: interlocus contrasts in the Northern acorn barnacle, *Semibalanus balanoides*. *Evolution*, 53, 135–146.

Schmidt PS, Serrao EA, Pearson GA, Riginos C, Rawson PD, Hilbish TJ, Brawley SH, Trussell GC, Carrington E, Wethey DS, Grahame JW, Bonhomme F, Rand DM (2008). Ecological genetics in the North Atlantic: environmental gradients and adaptation at specific loci. *Ecology*, 89, 91–107.

Simon A, Duranton M (2018) Digest: Demographic inferences accounting for selection at linked sites. *Evolution*, 72(6), 1330–1332.

Skibinski DOF, Beardmore JA, Cross TF (1983) Aspects of the population genetics of *Mytilus* (Mytilidae; Mollusca) in the British Isles. *Biol. J. Linn. Soc.*, 19, 137–183.

Smith SM, Maughan PJ (2015) SNP genotyping using KASPar assays. *Methods in Mol. Biol.*, 1245, 243–256.

Szulkin M, Gagnaire P-A, Bierne N, Charmantier A (2016) Population genomic footprints of fine-scale differentiation between habitats in Mediterranean blue tits. *Mol. Ecol.*, 25, 542–558.

Tine M, Kuhl H, Gagnaire P-A, Louro B, Desmarais E, Martins RST, Hecht J, Knaust F, Belkhir K, Klages S, Dieterich R, Stueber K, Piferrer F, Guinand B, Bierne N, Volckaert FAM, Bargelloni L, Power DM, Bonhomme F, Canario AVM, Reinhardt R (2014) European sea bass genome and its variation provide insights into adaptation to euryhalinity and speciation. *Nat. Comm.*, 5, 1–10.

Väinölä R, Hvilsom MM (1991) Genetic divergence and a hybrid zone between Baltic and North Sea *Mytilus* populations (Mytilidae: Mollusca). *Biol. J. Linn. Soc.*, 43, 127–148.

Van Belleghem SM, Rastas P, Papanicolaou A, Martin SH, Arias CF, Supple MA, Hanly JJ, Mallet J, Lewis JJ, Hines HM, Ruiz M, Salazar C, Linares M, Moreira GRP, Jiggins CD, Counterman BA, McMillan WO, Papa R (2017) Complex modular architecture around a simple toolkit of wing pattern genes. *Nat. Ecol. Evol.*, 1, 0052.

Weir BS, Clark Cockerham C (1984) Estimating F-Statistics for the Analysis of Population Structure. *Evolution*, 38, 1358.

Wong EH, Khrunin A, Nichols L, Pushkarev D, Khokhrin D, Verbenko, D, et al. (2017) Reconstructing genetic history of Siberian and Northeastern European populations. *Genome Res.* 27(1), 1–714.

Zeller KA, McGarigal K, Whiteley AR (2012) Estimating landscape resistance to movement: a review. *Landscape Ecology*, 27(6), 777–797.

Data Accessibility

Text S1. Pairwise F_{ST} values between Northern species at the GBS SNPs. (A) F_{ST} between Med and Nor; (B) F_{ST} between Med and Tva; (C) F_{ST} between Nor and Tva; Nor: North Sea *M. edulis*; Med: West-Mediterranean *M. galloprovincialis*; Tva: Baltic Sea *M. trossulus*.

Text S2. KASPar genotypes of each individual in the Kerguelen Islands (35 sampling sites), plus those of the additional individuals from other Southern Hemisphere populations (6 sampling sites).

Text S3. Individual ancestries estimated with ADMIXTURE for the GBS samples. (A) K=2; (B) K=3; (C) K=4; (D) K=5; (E) K=6; (F) K=7; (G) K=8.

Text S4. Individual ancestries estimated with ADMIXTURE for the KASPar samples in the Kerguelen (K=2; defining reference populations as *M. edulis* and Chilean mussels).

Text S5. Joint site frequency spectrum (in ∂a∂i format) between the Kerguelen mussels and (A) *M. edulis;* (B) *M. galloprovincialis*; (C) *M. trossulus*.

Text S6. Definition of the eight models of divergence used in our inferences with ∂a∂i.

Text S7. Neighbour-joining trees of the 395 retained GBS sequences.

Dryad doi: 10.5061/dryad.6k740. DNA sequences and VCF files including GBS genotypes of each individual in the ten GBS-typed populations (nine Northern populations and eight Kerguelen mussels).

Supplementary Information

Supplementary Information M&M

Supplementary Information Tables (S1 – S12)

Supplementary Information Figures (S1 – S8)

Supplementary Information Texts (S1 – S7)

Author Contributions

Data acquisition: A. Haguenauer, A. Weber and K. Gérard. *Data analysis*: C. Fraïsse, A. Chenuil and N. Bierne. *Writing*: C. Fraïsse, A. Chenuil and N. Bierne. *Conceptualization*: C. Fraïsse, A. Chenuil and N. Bierne. *Funding acquisition*: A. Chenuil and N. Bierne.

832 # Tables

Table 1. Counting the different gene topologies for the GBS dataset (10 populations, 67 gene trees)

topology	categories	counts	
		weight >= 0.90	weight >= 0.75
A. *M. edulis* with Kerguelen	A1 ancient Kerguelen divergence	3	5
	A2 introgression	5	12†
	NA	5	22
	total	**13**	**39**
B. *M. galloprovincialis* with Kerguelen	B1 ancient Kerguelen divergence	2	2
	B2 introgression	3	3
	NA	0	4
	total	**5**	**9**
C. *M. trossulus* with Kerguelen	C1 ancient Kerguelen divergence	5	11
	C2 introgression	3	4
	NA	1	4
	total	**9**	**19**
TOTAL		**27**	**67**

833 **topology**: three topologies have been weighted with *Twisst* (among the 395 gene trees, only 67 were topologically resolved); **categories**: "*ancient divergence*": the Kerguelen
834 population branched as a sister-clade to a Northern species; "*introgression*": Kerguelen mussels were distributed within a Northern species; "*na*": topologies that we were unable to
835 classify in these two categories. **weight**: exact weightings of each topology to the full tree.

Table 2. RDA analysis for the KASPar dataset (695 individuals, 33 SNPs)

	RDA (N=695)					conditioned RDA (N=695)			
	variance	%variance	d.f.	p-value		variance	%variance	d.f.	p-value
A. Global effect					**A. Environmental effect**				
Model	0.5288	2.324	7	0.001 ***	Substrate+*Macrocystis*+Slope	0.1213	1.0929	6	0.041 *
Residual	22.2183	97.676	687	-	Residual	10.9621	98.7588	687	-
B. Marginal effect					**B. Individual effect**				
Longitude	0.0128	0.0563	1	0.664	Longitude	0.1424	0.626	1	0.001 ***
Substrate	0.0594	0.261	3	0.133	Substrate	0.2322	1.021	3	0.001 ***
Macrocystis	0.0275	0.121	1	0.032 *	*Macrocystis*	0.0691	0.304	1	0.011 *
Slope	0.0379	0.167	2	0.217	Slope	0.0912	0.401	2	0.072 .
Residual	10.9621	48.191	687	-	Residual	22.2183	97.676	687	-

RDA significance tests are shown on the left for: (**A**) the global model with non-significant terms removed; and (**B**) the marginal effect of each constraining variable, which was tested through permutation tests by removing each term one by one from the model containing all other terms. Conditioned RDA significance tests are shown on the right for: (**A**) the combined effect of environmental variables after conditioning on Longitude; and (**B**) for each term after conditioning on other constraining variables to remove their confounding effects. **N**: number of individual genotypes; **variance**: genotypic variance explained by each factor; **%variance**: percent of genotypic variance; **d.f.**: degrees of freedom; **p-value**: p-values obtained through 1000 permutations (* ≤ 0.05; ** ≤ 0.01; *** ≤ 0.001).

Figures

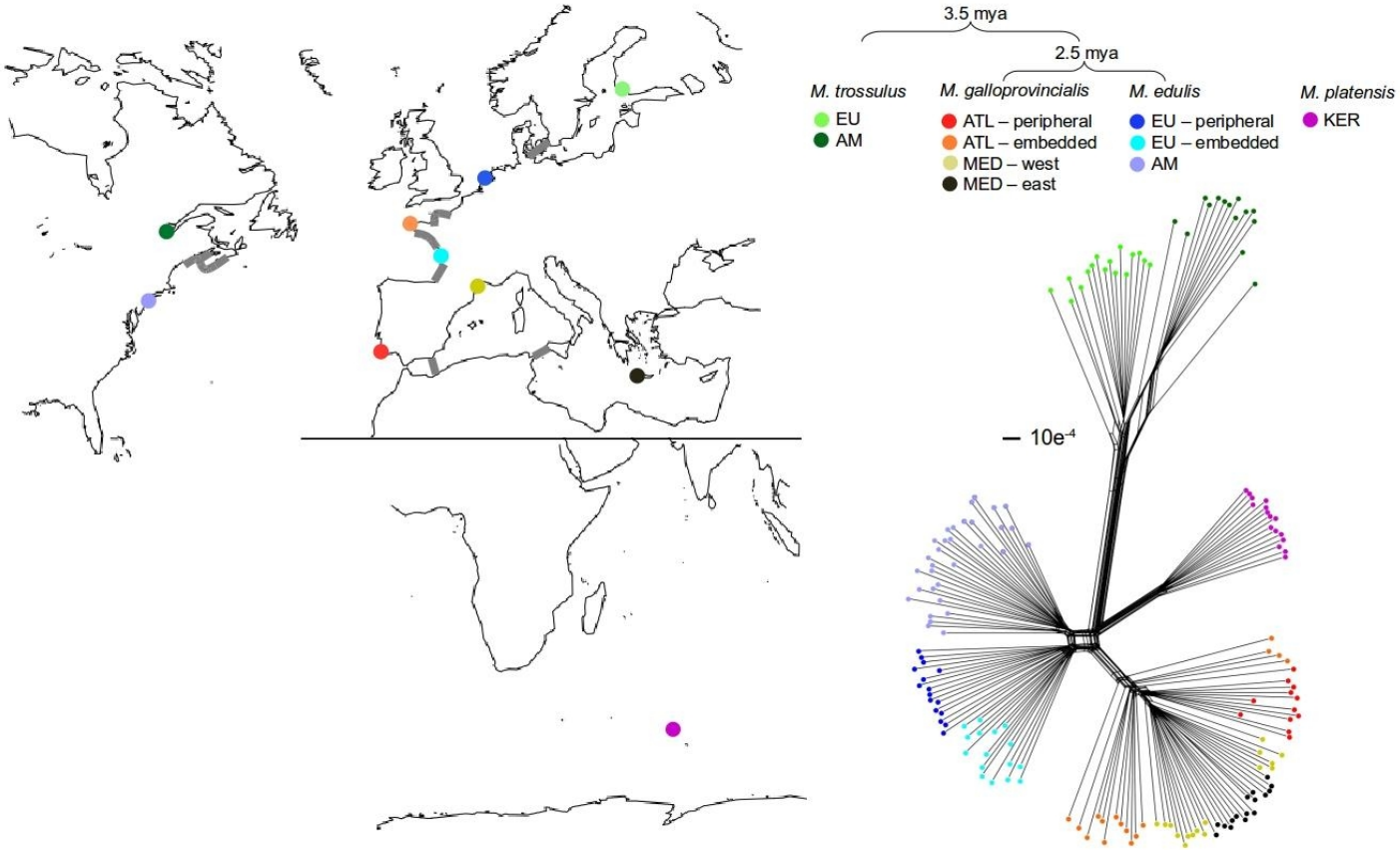

Figure 1. Localities and genetic network of the Northern and Southern *Mytilus* samples (ten GBS-typed populations). The genetic network was produced with the neighbour-net method based on 51,878 high-quality GBS SNPs. The *Mytilus platensis* sample is 'Baie de la Mouche' (KER, purple) in the Kerguelen Islands (Southern Ocean). *Mytilus trossulus* samples are 'Tvarminne' (EU, light green) in the European population of the Baltic Sea and 'Tadoussac' (AM, dark green) in the American population of the Saint Lawrence River. *Mytilus galloprovincialis* samples are 'Faro' (ATL – peripheral, red) in the Atlantic population of Iberian Coast, 'Guillec' (ATL – embedded, orange) in the Atlantic population of Brittany, 'Sete' (MED – west, yellow) in the Occidental Mediterranean basin and 'Crete' (MED – east, black) in the Oriental Mediterranean basin. *Mytilus edulis* samples are 'Wadden Sea' (EU – peripheral, light blue) in the European population of the North Sea, 'Lupin/Fouras' (EU – embedded, cyan) in the European population of the Bay of Biscay and 'Quonochontaug/Old Saybrook Town' (AM, slate blue) in the American population of Rhode Island. Estimate of divergence times between Northern species are indicated with braces (Rawson & Hilbish 1995 , Roux *et al.* 2014), and contact zones between them are depicted by grey stripes.

Figure 2. Evidence of admixture in the ten GBS-typed *Mytilus* spp. populations. **A.** Maximum-likelihood population tree inferred by *TreeMix* showing 7 migration events. ML estimation was made by using 32,162 GBS SNPs grouped in windows of 100 SNPs. Terminal nodes are labelled by locality abbreviation (Figure 1 and Table S1) and colors match Figure 1. The drift parameter is shown on the x-axis. Horizontal branch lengths are proportional to the amount of genetic drift that has occurred in each branch. Admixture arrows are coloured according to the migration weight, which represents the fraction of ancestry derived from the migration event. Migration events with bootstrap support less than 50% are shown with dotted lines, and those with bootstrap support less than 20% are not shown (Table S8). **B.** Pairwise privately shared SNPs between a subset of populations of similar sample size (Table S1). The width of the lines is proportional to the number of SNPs shared (*M. trossulus:* KER-AM=1,394 (America); *M. galloprovincialis*: KER-ATL=254 (Atlantic - peripheral) and KER-MED=392 (Occidental Mediterranean basin); *M. edulis*: KER-EU=421 (Europe - peripheral) and KER-AM=532 (America)). The size of the circles is proportional to the number of non-shared private SNPs (KER=6,022; *M. trossulus*: AM=13,095; *M. galloprovincialis*: ATL=1,948, MED=3,927; *M. edulis*: EU=3,251, AM=2,731). Singletons were removed.

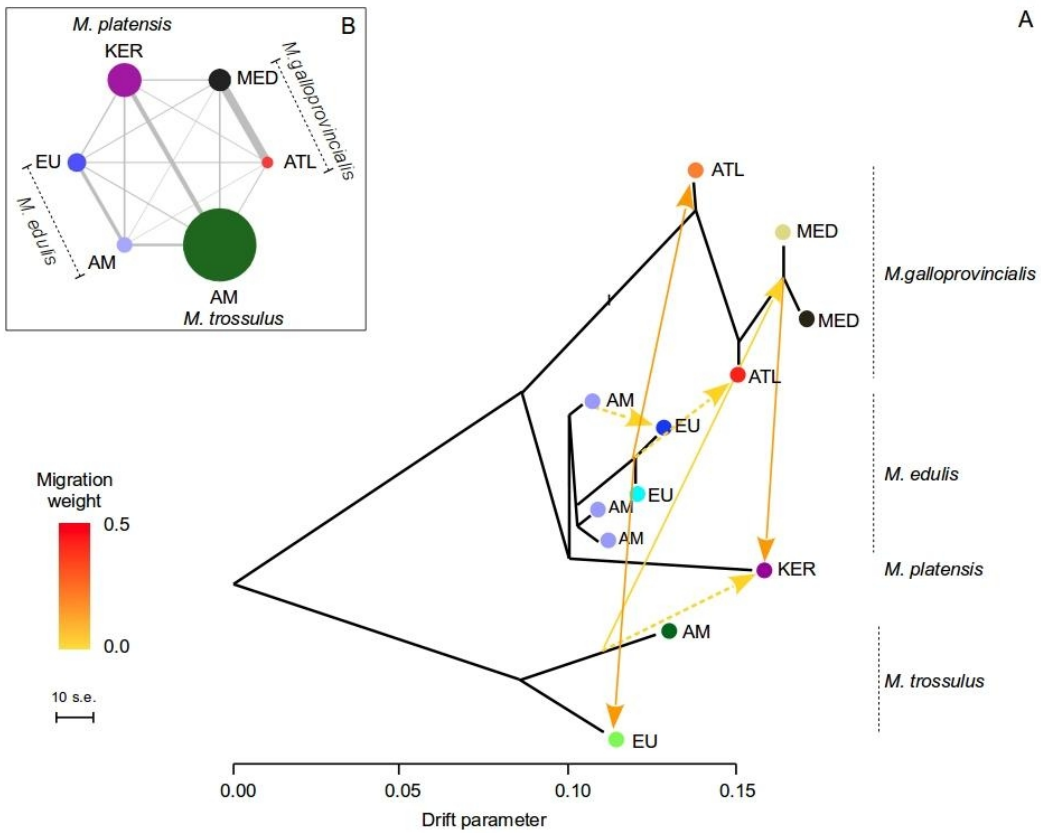

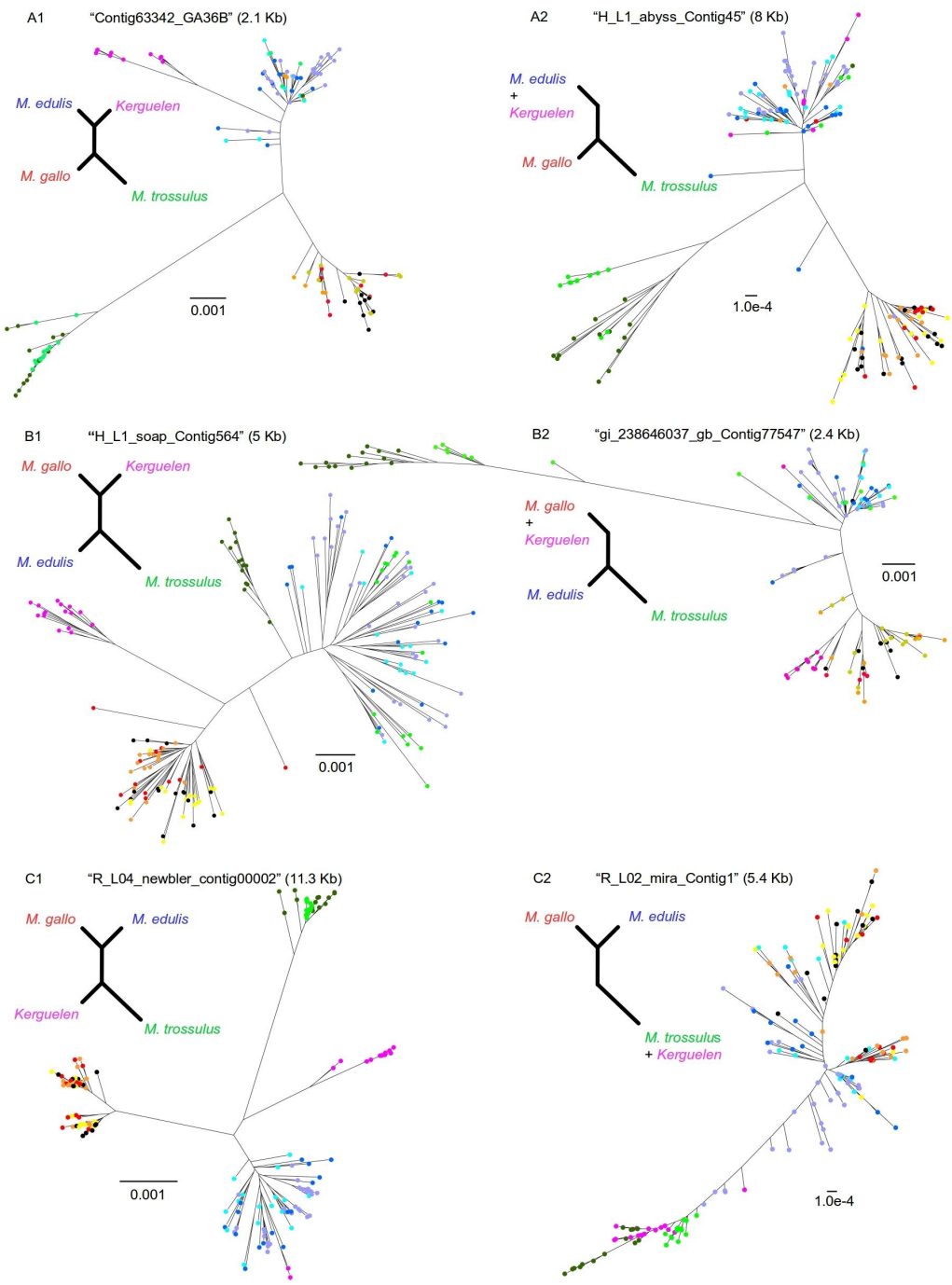

Figure 3. Summary of the different gene topologies obtained with *Twisst* for the GBS dataset. Three topologies have been weighed with *Twisst* for each of the 395 contigs (of which only 67 were topologically resolved), and classified in different categories depending whether the Kerguelen mussels branched as a sister-clade to a Northern species ("ancient divergence"), or were distributed within a Northern species ("introgression"). **A.** Kerguelen clustered with *Mytilus trossulus*: A1 "ancient Kerguelen divergence" and A2: "introgression"; **B.** Kerguelen clustered with *Mytilus edulis*: B1 "ancient Kerguelen divergence" and B2: "introgression"; **C.** Kerguelen clustered with *Mytilus galloprovincialis*: C1 "ancient Kerguelen divergence" and C2: "introgression". For each category, a typical neighbour-joining tree computed on the longest non-recombining block of the contig is shown (defined with the Difference of Sums of Squares method of McGuire & Wright 2000). In panel A2, the *Mytilus edulis* haplotypes have totally replaced their Southern counterparts in the Kerguelen. Panel B2 suggests a more ancient introgression of *Mytilus galloprovincialis* haplotypes given that all haplotypes sampled in the Kerguelen form a distinct cluster within the *Mytilus galloprovincialis* clade. And panel C2 represents a complete introgression of *Mytilus trossulus* haplotypes into the Kerguelen. Contig IDs correspond to Table S6, and sizes of non-recombining blocks are given in brackets. Colors match Figure 1.

Figure 4. Geographic variation of the average foreign allele frequency across the four most differentiated loci in the Kerguelen Islands (filled symbols, X10, X11, X57 and Glu-5' from Gérard *et al. (*2015)) and the other loci (open symbols). Alleles were labelled based on their frequencies in the *M. galloprovincialis* Atlantic population of Iberian Coast (Table S4). Red points indicate sites located in the Gulf of Morbihan. **A.** Map of the Kerguelen Islands (150 km East to West; 120 km North to South) together with a world map indicating its location in the Southern Ocean (surrounded in red), and an enlarged map of the Henri Bossière Fjord. Sites PAF (the main harbour of the island) and RdA are separated by 40 kms of coasts, RdA and Pmo by 8 kms, and they show a genetic break on Panel B. Sampling details are provided in Table S3. **B.** Frequency of the average foreign allele across sampling sites in the Kerguelen Islands (ordered by geography), in the three reference Northern species and in the Chilean mussels. See Figure S4 for the detailed pattern at each locus. On top, the average *Mytilus edulis* vs. Chilean ancestries from an ADMIXTURE analysis (K=2) are shown for each site. **C.** Simulation results after 300 generations of a secondary contact between *Mytilus edulis* and Chilean *Mytilus platensis* mussels that meet twice on a circular stepping-stone model (between demes n°18 / n°19 and demes n°19 / n°20). A physical barrier to dispersal was modelled between the *Mytilus edulis* deme (n°19) and the Chilean deme n°18 (dashed vertical bar, migration rate=0.05 instead of 0.5 as everywhere else). Deme size was fixed to 500 individuals, and the species barrier was asymmetric (at barrier loci, the selection coefficient against *Mytilus edulis* in the *Mytilus platensis* background was set to 0.2 while it was set to 0.5 against the *Mytilus platensis* allele in the *Mytilus edulis* background).

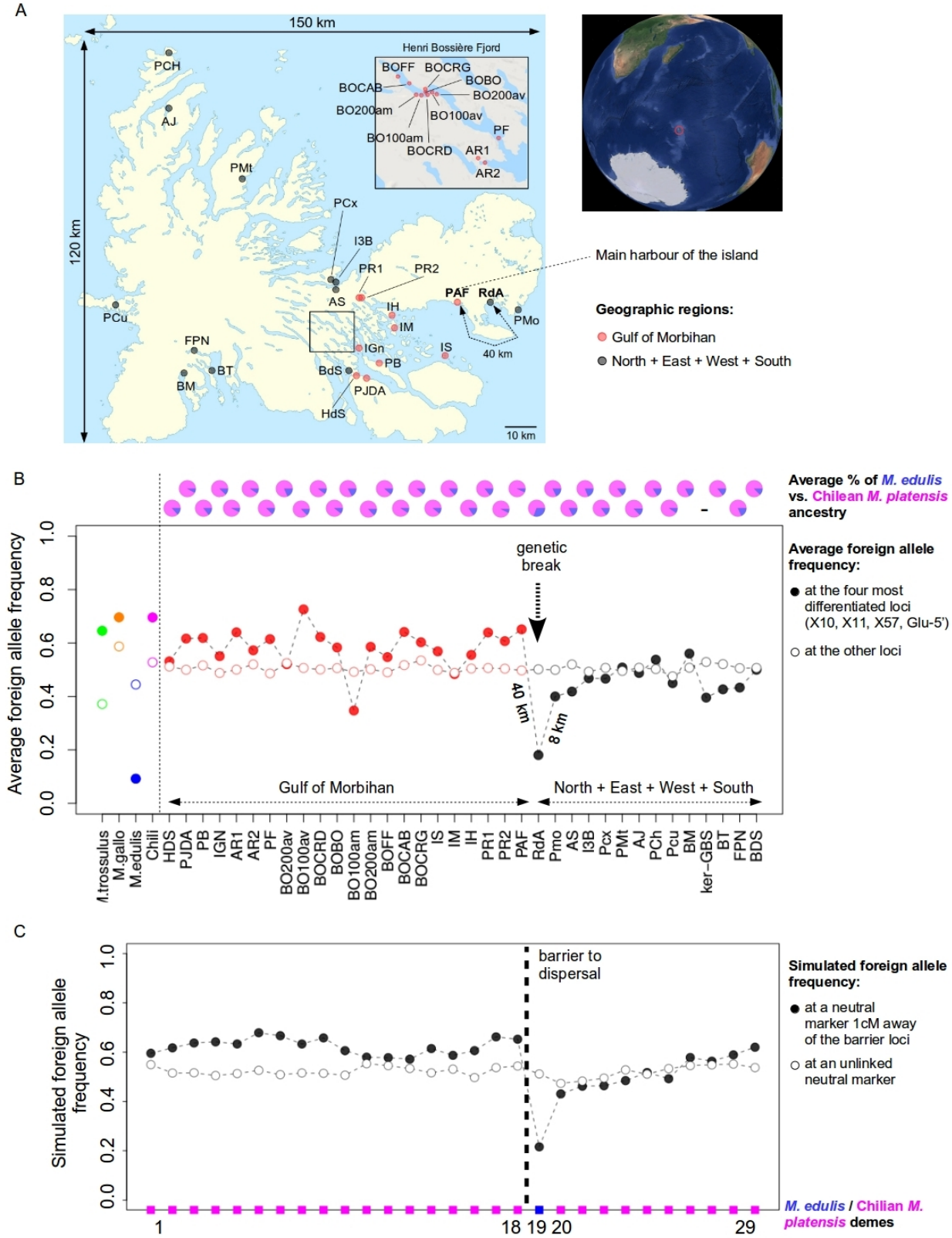
A
150 km
120 km
Henri Bossière Fjord
BOFF
BOCRG
BOCAB
BOBO
BO200av
BO200am
BO100av
BO100am
BOCRD
PF
AR1
AR2
PCH
AJ
PMt
PCx
I3B
PR1
PR2
AS
PAF
RdA
IH
IM
PMo
PCu
FPN
IGn
IS
40 km
BT
BM
BdS
PB
PJDA
HdS
10 km
Main harbour of the island
Geographic regions:
Gulf of Morbihan
North + East + West + South
B
Average % of M. edulis vs. Chilean M. platensis ancestry
Average foreign allele frequency
genetic break
Average foreign allele frequency:
at the four most differentiated loci (X10, X11, X57, Glu-5')
at the other loci
40 km
8 km
Gulf of Morbihan
North + East + West + South
M.trossulus
M.gallo
M.edulis
Chili
HDS
PJDA
PB
IGN
AR1
AR2
PF
BO200av
BO100av
BOCRD
BOBO
BO100am
BO200am
BOFF
BOCAB
BOCRG
IS
IM
IH
PR1
PR2
PAF
RdA
Pmo
AS
I3B
Pcx
PMt
AJ
PCh
Pcu
BM
ker-GBS
BT
FPN
BDS
C
Simulated foreign allele frequency
barrier to dispersal
Simulated foreign allele frequency:
at a neutral marker 1cM away of the barrier loci
at an unlinked neutral marker
1
18 19 20
29
M. edulis / Chilian M. platensis demes

Figure 5. Correlation between the average foreign allele frequency of the four most differentiated loci (**A**) and other loci (**B**) at each sampling site in the Kerguelen Islands (y-axis, Table S4), and the presence/absence of *Macrocystis* (x-axis, this is the average sampling site coordinates on the first axis of the *Macrocystis* RDA, see Table S12). Pearson correlation coefficient: on the left panel, 0.494 (p-value=0.003); on the right panel, 0.107 (p-value=0.541). Red points indicate sites located in the Gulf of Morbihan (see Figure 4A).

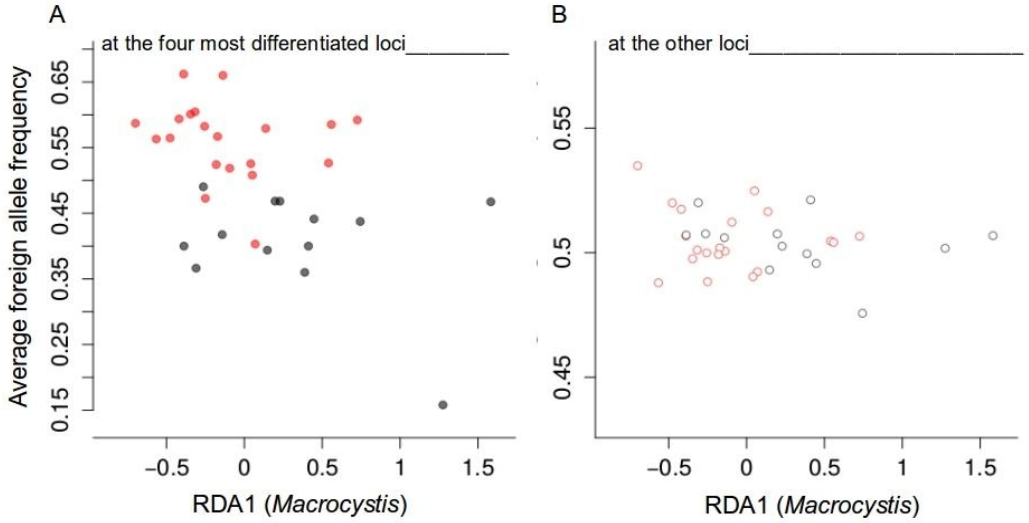
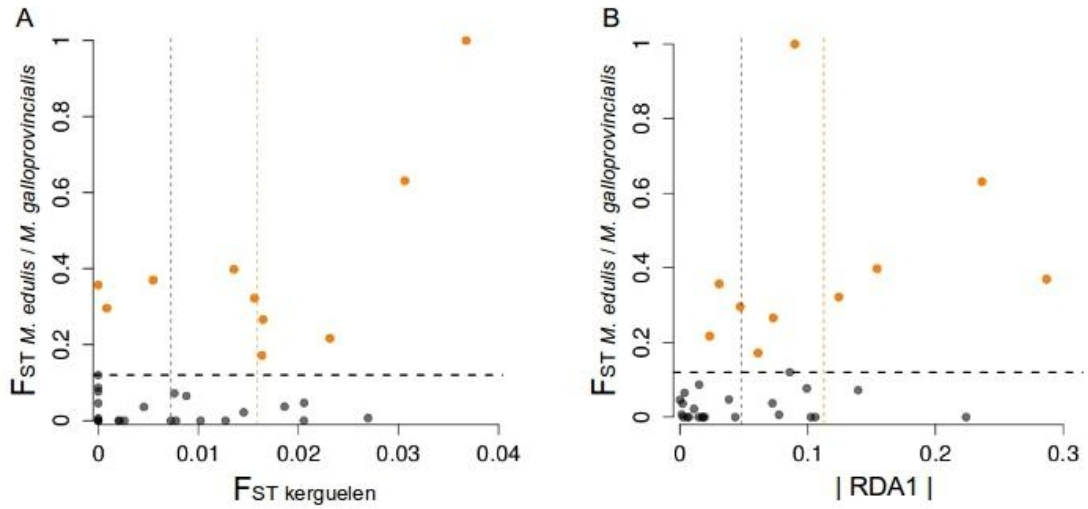
Figure 6. Correlation between the level of differentiation among the Kerguelen Islands (x-axis) and the Northern species (F_{ST}, y-axis) at each KASPar SNP. Panel (**A**) shows the genetic differentiation between Kerguelen populations (global F_{ST}); and panel (**B**) shows the genetic-by-environment association (locus coordinates on the first axis of the conditioned RDA (absolute values), see Table S11). Northern species are *Mytilus edulis* (EU – peripheral, European population of the North Sea) and *Mytilus galloprovincialis* (MED - west, Mediterranean population of the West basin). Ancestry-informative loci, i.e., F_{ST} *M.edulis_M.galloprovincialis* > 0.120 (horizontal dashed line, see Table S2), are depicted in orange. Wilcoxon's test between the ancestry-informative loci (orange) and the background loci (grey): (**A**) mean_orange=0.015, mean_grey=0.007 (p-value=0.021); (**B**) mean_orange=0.112, mean_grey=0.048 (p-value=0.006). Their respective means are depicted by vertical dashed lines. Pearson correlation coefficient: (**A**) r=0.540 (p-value=0.001); (**B**) r=0.439 (p-value=0.011).